SEISMIC BEHAVIOUR OF GROUTED SLEEVE PRECAST COLUMN TO FOUNDATION CONNECTIONS: RESULTS APPLIED TO THE DIRECT DISPLACEMENT BASED DESIGN

A. Belleri[1] and P. Riva[2]

[1] *Graduate Student, Dept. of Design and Technology, University of Bergamo, Dalmine. Italy*
[2] *Professor, Dept. of Design and Technology, University of Bergamo, Dalmine. Italy*
Email: andrea.belleri@unibg.it, paolo.riva@unibg.it

ABSTRACT :

In this paper we present the application of Direct Displacement Based Design (DDBD) to precast concrete structures with different column to foundation connections, whose structural response has been obtained through a set of experimental tests carried out at the University of Brescia, involving cast in place, pocket foundation and grouted sleeve solutions. The latter have a slightly smaller dissipation capacity while being able to ensure a similar ductility, compared to the other solutions; the main advantage is to limit the damage to the grout layer between the precast column and the foundation. The experimental data allowed to calibrate the moment-curvature hysteretic parameters used in the finite elements analyses carried out to validate the DDBD procedure. The analyses results of structures designed according to DDBD procedure show a lack of accuracy in the maximum displacement predicted by the design procedure; a better estimation of the structural yielding displacement and the development of a procedure, based on inelastic spectra analyses, to recalibrate the hysteretic damping equations available in the literature allowed to improve the maximum displacement prediction. This procedure is suitable for other hysteretic models calibration.

KEYWORDS: precast column, column-foundation joint, DDBD, hysteretic damping

1. INTRODUCTION

Precast concrete structures have been widely used in Italy since the 1950s due a the sensible reduction in the construction time, the cost effectiveness and the better plant control of structural elements and materials compared to on site constructions. The most common applications of precast buildings in Italy are in the industrial and commercial sectors, likewise warehouses and commercial malls respectively. The typical structural layout consists of cantilever columns, connected by simply supported precast and prestressed beams, supporting prestressed concrete roof elements; the columns are inserted and grouted in place in isolated precast cup-footings. The seismic design of these structures is usually carried out neglecting the moment capacity between the top column and the supporting beam connections. Adopting seismic design criteria based on the building performance, like maximum displacement and deformation as in the DDBD procedure, rather than the ultimate resisting force, as in the Force Based Design (FBD) procedure, we note how the target displacement ductility associated to the typical precast concrete structures is lower than the one associated to other reinforced concrete structures; this is due to the larger interstory height of precast structures compared to normal cast in situ buildings. We note that the low amount of ductility required leads to a limit state related to the interstory drift control rather than to a material strain limit requirement.
The DDBD procedure (Sullivan et al. 2005) has been optimized and the hysteretic damping equation calibrated only for a limited amount of hysteretic models. In particular, regarding reinforce concrete buildings, the procedure has been calibrated only for structures whose substitute structure force-displacement behavior is well described by two sets of Takeda hysteretic model parameters, the "Takeda fat" and "Takeda narrow" models (Grant et al. 2004). The purpose of this paper is to explore how the DDBD procedure behaves and how can be improved when applied to structures whose hysteretic behavior is slightly different from the ones available in the literature, like in the case of precast concrete structures with different column to foundation connections.

The case study under consideration is a one story 6x7 bays precast concrete building whose plan dimensions are 76 and 87 m. The structure can be modelled as a set of cantilever column connected at the top by pinned elements as part of a rigid diaphragm. Therefore we can analyze a single column (H=7.9 m: height of roof mass centroid) with the mass (m=82946 kg: corresponding to the tributary area) concentrated at the column top; the target drift chosen is 2.5% (Δ_d=0.1975 m). The materials adopted are concrete C40/50 and steel B430C; the seismic design has been done according to EC8-1:2004 type 1 spectrum, soil type C and a peak ground acceleration of 0.5 g.
The ground motions used to validate the results in the non linear time history (NLTH) analyses are the ones selected by the line 4 of the RELUIS national project (Table 1).

Table 1. Ground motions adopted

Earthquake station	Duration (s)	Scale factor
Duzce	25.89	1.2
Kalamata	29.995	3.1
Kocaeli– 1	70.38	2.1
Northridge–Baldwin	60.00	4.5
Hella	60.00	2.0
SIMQKE 1	19.99	artificial record
SIMQKE 2	19.99	artificial record

2. DIRECT DISPLACEMENT BASED DESIGN PROCEDURE

The DDBD procedure (Sullivan et al. 2005), adopting a substitute structure approach, starts with the definition of the structural deformed shape (Δ_i), linear in this case, and with the choice of the target displacement (Δ_d), which in this case is related to the interstory drift value. With these two definitions, we can define the single degree of freedom (SDOF) substitute structure and get its effective height (H_{eff}) and mass (m_{eff}) through Eqns. 2.1 and 2.2:

$$H_{eff} = \frac{\sum_{i=1}^{n} m_i \Delta_i H_i}{\sum_{i=1}^{n} m_i \Delta_i}, \qquad m_{eff} = \frac{\sum_{i=1}^{n} m_i \Delta_i}{\Delta_d} \qquad (2.1)\ (2.2)$$

The next step consists in the determination of the equivalent viscous damping, adopted by DDBD to represent the elastic and the hysteretic damping $\xi_{eq}=5\%+\xi_{hyst}$; the first term, the elastic viscous damping, takes into account different sources of damping like material viscous damping and radiation damping due to the foundation system, while the second term, the hysteretic damping, depends on the hysteretic relationship of the structural elements and takes into account the capacity of the system to dissipate energy.
The equivalent viscous damping value is used to determine the design displacement spectrum reduction for damping values different from 5%. This reduction has been evaluated by means of a least square procedure for the ground motions adopted, instead of using the general EC8 formula, because we wanted to eliminate this source of uncertainty from the analyses. Therefore the equation which better describes the dependence of damping of the mean displacement spectrum in the period range 0-2 s is (Eqn. 2.3):

$$\frac{SD(\xi)}{SD(5\%)} = \sqrt{\frac{7.8}{2.8+\xi_{eq}}}. \qquad (2.3)$$

With the displacement spectrum so reduced, we can evaluate the substitute structure effective period associated to the target displacement, and from that the effective stiffness associated to the substitute structure maximum response. The design base shear is equal to (Eqn. 2.4):

$$V_b = k_{eff}\Delta_d = 4\pi^2 \frac{m_{eff}}{T_{eff}^2}\Delta_d. \qquad (2.4)$$

The equivalent viscous damping formulation used in this study is the one described by Grant et al. (2004), which relates the equivalent viscous damping to the target system ductility ($\mu_\Delta = \Delta_d/\Delta_y$) and to the substitute structure effective period. The yield displacement Δ_y for the structure under consideration is the one associated to a linear variation of the curvature along the column height from zero to the yield curvature ϕ_y (Priestley 2003), which leads to (Eqn. 2.5):

$$\Delta_y = \phi_y \times \frac{H^2}{3} = 2.1\frac{\varepsilon_y}{h} \times \frac{H^2}{3}. \tag{2.5}$$

Where h, H and ε_y are the cross-section depth the column height and the steel yield strain respectively.
The equivalent viscous damping formula (Eqn. 2.6) is:

$$\xi_{eq} = 0.05 + a\left(1 - \frac{1}{\mu_\Delta^{\ b}}\right)\left(1 + \frac{1}{\left(T_{eff} + c\right)^d}\right) \tag{2.6}$$

The previous parameters (a,b,c and d) have been calibrated for different hysteretic models (Grant et al. 2004): the one adopted for this study is the Takeda model whose force-displacement relationship is described by $\alpha = 0.3$, $\beta = 0.6$, $r = 0.05$ (Figure 1); the corresponding parameters for design purposes (Eqn. 2.6) are $a = 0.249$, $b = 0.527$, $c = 0.761$ and $d = 3.250$ (Takeda "fat" model). The procedure adopted in the aforementioned work to calibrate Eqn. 2.6 is based on the force-displacement response of SDOF systems, while in this research the Takeda model is used to describe the column moment-curvature response. Therefore we need to define the relationship between the parameters for the force-displacement and moment-curvature Takeda models (Figure 1).

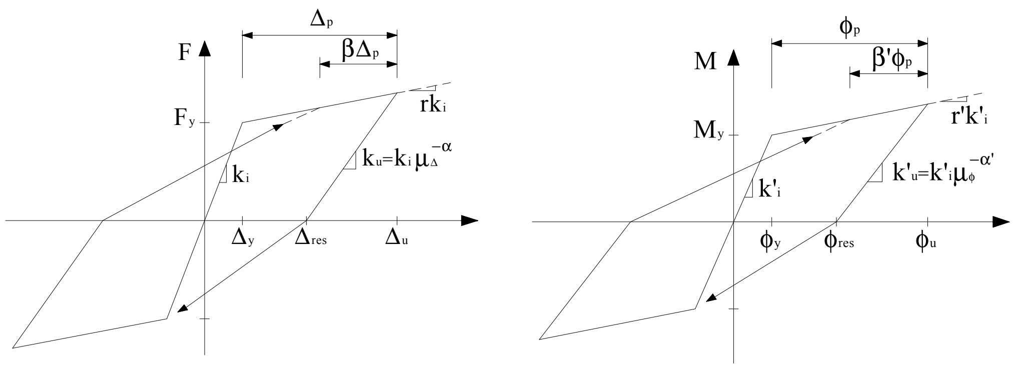

Figure 1. Force-Displacement and Moment-Curvature Takeda models.

According to the notation in Figure 1, the relationship between parameter r and r', β and β' and between curvature and displacement ductility, considering a plastic hinge region of length L_p with constant plastic curvature ϕ_p located at the element ends, are respectively (Eqns. 2.7, 2.8, 2.9):

$$r = r'\frac{H}{3L_p}; \quad \beta = \beta'; \quad \mu_\phi = \frac{\phi_u}{\phi_y} = 1 + \frac{\mu_\Delta - 1}{r' + 3\frac{L_p}{H}(1 - r')}. \tag{2.7) (2.8) (2.9}$$

The relationship between α and α' is (Eqn. 2.10):

$$\alpha' = \left\{ \ln\left[-\frac{H}{3L_p} + 1 + \frac{H}{3L_p}\mu_\Delta^{\alpha}\left[1 + r'\left(\mu_\phi - 1\right)\right]\right] - \ln\left[1 + r'\left(\mu_\phi - 1\right)\right]\right\}\frac{1}{\ln\left(\mu_\phi\right)} \tag{2.10}$$

Based on the previous considerations, we applied the DDBD procedure to the case study and we carried out a set of NLTH analyses of columns whose moment-curvature relationship ideally matched the one of the "Takeda fat" model, whose hysteretic damping equation parameters are available in the literature.
The drifts obtained for different cross section sizes are represented in Figure 2, where we can see how the DDBD procedure succeeds in controlling both the mean and maximum displacements in a stable trend.

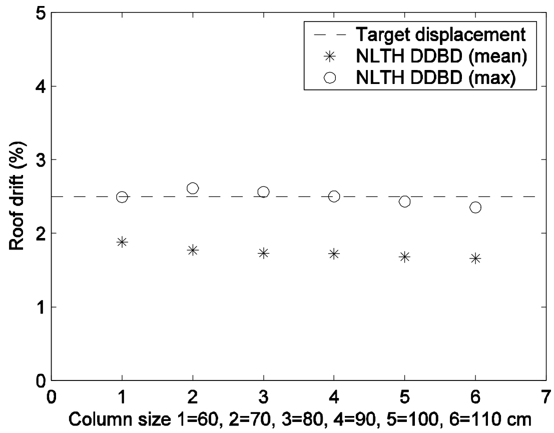

Figure 2. NLTH analyses mean and maximum roof drift.

In the following chapter we will analyze how the DDBD procedure behaves in the case of different hysteretic model parameters due to different column to foundation connections.

3. COLUMN TO FOUNDATION CONNECTION TESTS AND DDBD APPLICATION

The experimental tests concerned five specimens with different column to foundation connections and approximately the same maximum bending moment capacity. All the specimens tested had a 400x400mm column cross section and a clear height from the foundation to the top equal to 3200mm.
Specimens CS and PF are representative of a typical Cast in Situ column to foundation connection and grouted Pocket Foundation respectively; specimens GS4 and GS4B are both characterized by having four Grouted Sleeves with different anchorage length of the 26mm diameter bars in the foundation: the former has straight anchored bars, whereas the latter has 90° hooks at the bar ends. Specimen GS4U is like GS4B but with 300 mm of unbonded length for the 26mm diameter bars in the column.
For all the tests, the axial force, equal to 600kN, was first applied by means of two hydraulic jacks. A cyclic horizontal displacement history was then applied to the column top by means of a 1000 kN electromechanical screw jack.

In the following Figure 3 we show the specimens geometry and the comparison between the experimental and finite element model moment-drift curves. The moment-curvature relationship has been calibrated on the Takeda model hysteresis rule with the parameters shown in the figure.

Applying the DDBD procedure, without modifications, to columns whose base moment-curvature relationships are described by these sets of Takeda model parameters leads to the results presented in Figure 4, where we can see how the DDBD procedure does not properly control the maximum top displacement.

This is due to two reasons: the first one is that Eqn. 2.5 (yield displacement evaluation) is not suitable to describe the behavior of these particular connections; the second one is linked to Eqn. 2.6 (equivalent viscous damping) whose "Takeda fat" model parameters do not properly reflect the hysteretic damping associated to the different column to foundation connections. The improvement to these two drawbacks will be described in the next chapter.

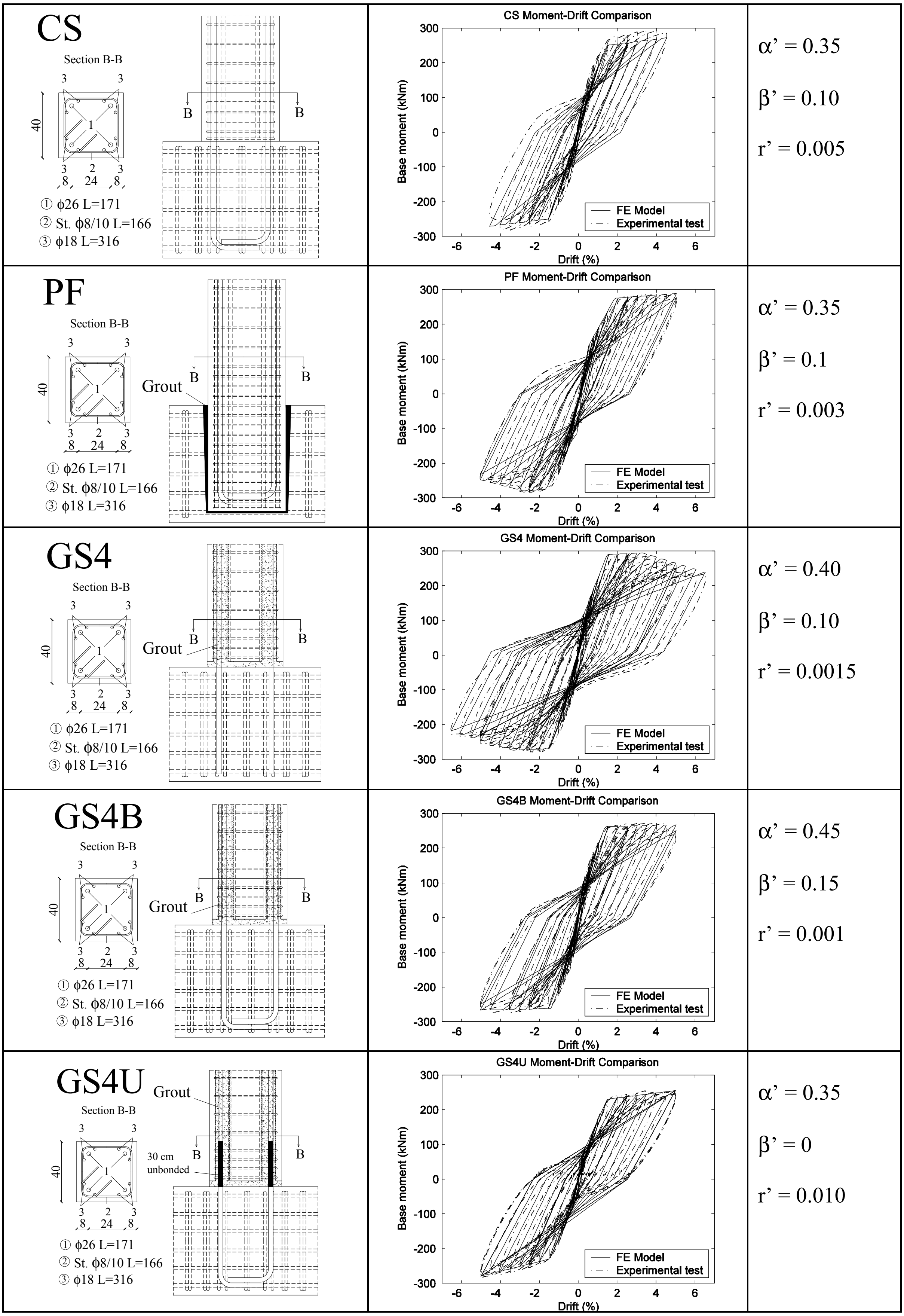

Figure 3. Experimental test geometry and moment-curvature finite element calibration.

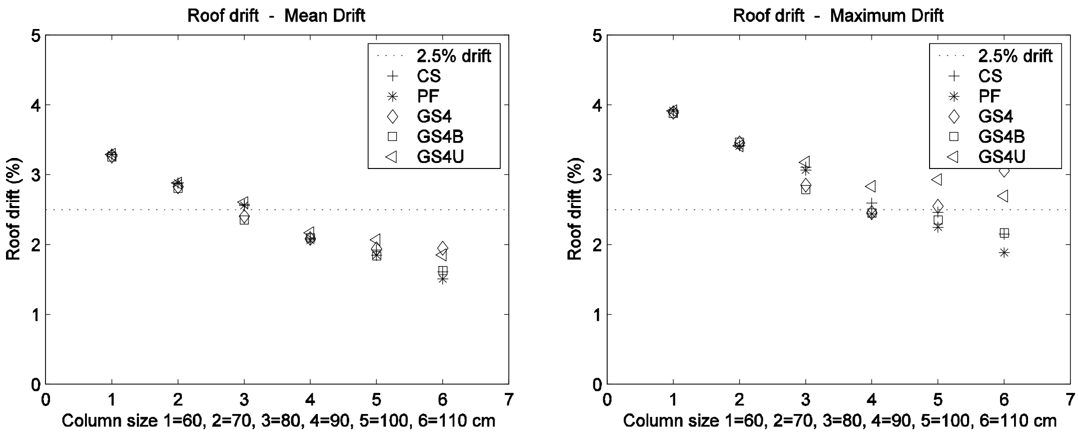

Figure 4. NLTH analyses mean and maximum roof drift.

4. DDBD PROCEDURE ENHANCEMENT

The first drawback stated in the previous chapter can be easily overcome observing that the yield curvature estimation (Priestley 2003) in Eqn. 2.5 has been derived from the moment-curvature relationships of square columns with flexural reinforcement evenly distributed along the perimeter, whose cross section size was 160 cm and the flexural reinforcement cover 5 cm, while in the experimental tests of Figure 3 the column dimensions was 40 cm and the distance between the foundation to column flexural reinforcement centre and the column edge was 8 cm. We note how, in the latter case, the ratio between the effective height and the column dimensions is significantly less than the former, which is close to unity. We observe how substituting the effective height (d) instead of the column cross section size (h) in Eqn. 2.5 leads to a yield displacement compatible with the experimental tests. Therefore the new yield curvature adopted in this study is (Eqn. 4.1)

$$\phi_y = 2.1\frac{\varepsilon_y}{d}. \tag{4.1}$$

As for the second drawback, we can get a new calibration of Eqn. 2.6 parameters to better reflect the hysteretic damping associated with different column to foundation connections.
The procedure adopted to calibrate the hysteretic damping expression available in literature (for a more detailed explanation refer to Grant et al. 2004) starts from the arbitrary choice of the SDOF system effective period, mass, yield displacement and displacement ductility, which allow to calculate the system maximum displacement and the initial and effective stiffness. After the definition of a first trial hysteretic damping, it is possible to determine the ground motion scaling factor such that the maximum inelastic displacement obtained from the time history analyses is equal to the maximum displacement predicted. Then, considering a linear elastic SDOF system whose stiffness is the effective stiffness and the damping associated is the one corresponding to the first trial equivalent viscous damping, it is possible to determine the new hysteretic damping such that the equivalent linear system reaches the maximum predicted displacement under the ground motions previously scaled, iterating with time history analyses and using Regula Falsi and bisection method.

The procedure proposed in this study, which we applied to the Takeda hysteretic model but can be easily extended to other hysteretic models, is based on the analysis of the force displacement inelastic response of single degree of freedom systems and it is articulated as following:

1. Choose the Force-displacement Takeda hysteretic model parameters whose hysteretic damping relationship we want to calibrate (in this case we used the parameters based on the experimental tests, Figure 3, and on Eqns. 2.7 through 2.10).
2. Obtain the inelastic spectra associated with the hysteretic model for a determined ductility range (in this case μ_Δ = 1.5, 2.0, 3.0, 4.0). These inelastic spectra refer to the SDOF systems elastic period, while Eqn. 2.6 refers to the effective period. The elastic and effective period relationship (Eqn. 4.2) can be obtained considering Figure 1:

$$T_{eff} = T\sqrt{\frac{\mu_\Delta}{1+r(\mu_\Delta - 1)}} \tag{4.2}$$

3. The hysteretic damping (Eqn. 4.3) is found by subtracting the elastic viscous damping value from the equivalent viscous damping obtained inverting Eqn. 2.3:

$$\xi_{hyst} = \xi_{eq} - 5 = \left(7.8\times\left(\frac{SD(5\%)}{SD(\xi)}\right)^2 - 2.8\right) - 5 = 7.8\times\left[\left(\frac{SD(5\%)}{SD(\xi)}\right)^2 - 1\right] \tag{4.3}$$

4. Eqn 2.6 parameters are finally obtained by means of least square regression using the downhill simplex algorithm (Nelder and al. 1965), based on the average value of the ground motion inelastic spectra.

The results of the calibration procedure for the different types of Takeda hysteretic models considered are summarized in Table 2, while Figure 4 represents the hysteretic damping relationship associated with these new parameters. Finally Figure 5 shows the results from the application of the DDBD procedure with the modification of Eqn. 2.5 and 2.6 stated before.

Table 2. New hysteretic damping parameters

	a	b	c	d
CS	0.511	0.143	0.677	0.692
PF	0.432	0.180	0.705	0.685
GS4	0.350	0.226	0.719	0.681
GS4B	0.333	0.238	0.721	0.680
GS4U	2.356	0.027	0.634	0.703

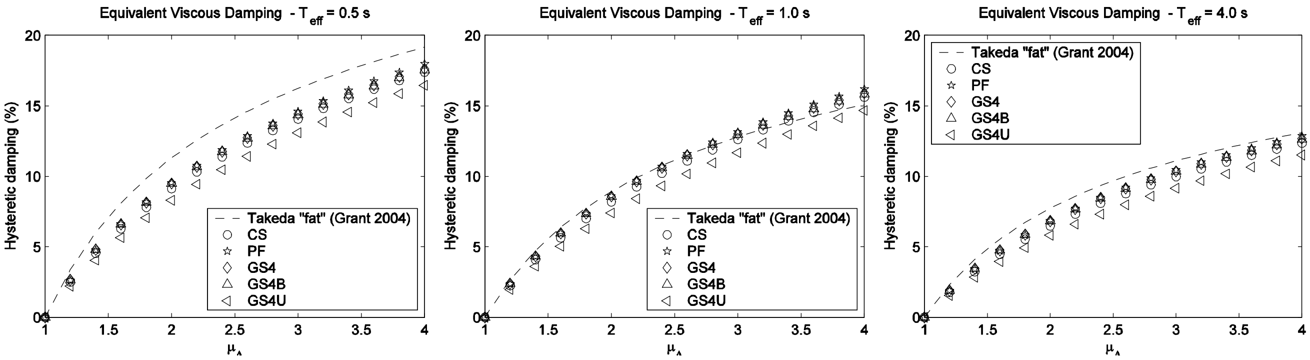

Figure 4. Effective period and displacement ductility hysteretic damping relationship.

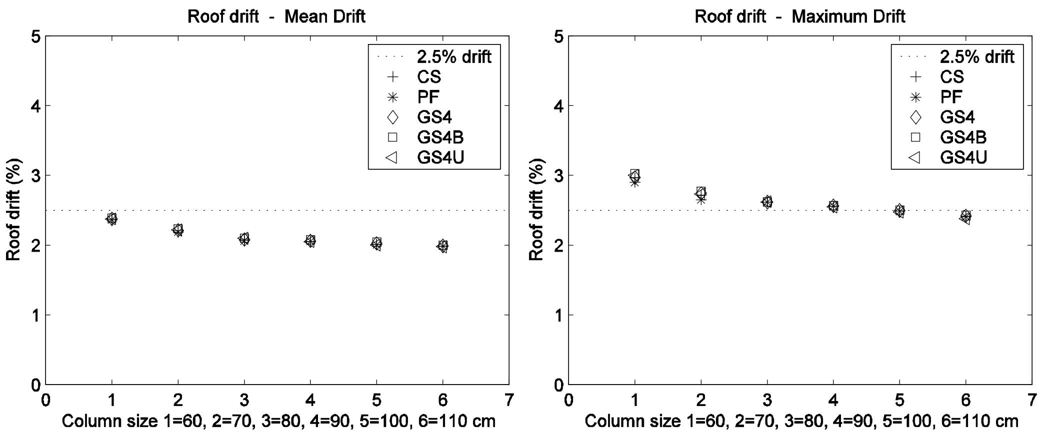

Figure 5. NLTH analyses mean and maximum roof drift.

We observe the good agreement between the design prediction and the NLTH analyses. We note that in this particular case the results are more affected by the modification of Eqn. 2.5 than Eqn. 2.6. In fact, the displacement ductility and the effective period of the structure under examination are about 1.2 and 1.1s respectively: these values lead to an hysteretic damping close to the one associated to the "Takeda fat" model available in the literature, as it is shown in Figure 4.

5. CONCLUSIONS

In this paper we explored the application of DDBD procedure on precast concrete structures with different column to foundation connections, whose behavior has been experimentally tested.
We observed how the DDBD application does not succeed in predicting the inelastic displacements; this is due to an improper estimation of both the yield curvature and the hysteretic damping associated to the different types of connections.
The first drawback is overcome by substituting the effective height instead of the column cross section size in the yield curvature definition (Eqn. 2.5).
Regarding the second drawback, the authors proposed a general procedure to determine the hysteretic damping associated to different types of hysteretic models used in finite element analysis.
The results show good agreement between the DDBD procedure predictions and the NLTH analyses results.

ACKNOWLEDGMENTS

This study has been supported by the DPC-Reluis national program within the framework of Research line 4: "Development of displacement-based approaches for the design and assessment of structures". The experimental tests have been financed by Moretti SpA (Erbusco –Italy) to study precast column to foundation connections.

REFERENCES

AA.VV. (2003). Seismic design of precast concrete building structures, *International Federation for Structural concrete*, bulletin 27

Belleri, A. and Riva, P. (2008). Direct Displacement Based Design and Force Based Design of Precast Concrete Structures, *Proceedings of the First International Symposium on Life-Cycle Civil Engineering*,

Blandon, C.A. and Priestley, M.J.N. (2005). Equivalent Viscous Damping Equations for Direct Displacement Based Design, *Journal of Earthquake Engineering*, **9: Special Issue 2**, 257-278.

Carr, A. J. (2004). Ruaumoko – Finite element program, University of Canterbury, Christchurch, New Zealand.

Eurocode 8-2004. Design of Structures for Earthquake Resistance, Part 1: General rules, seismic actions and rules for buildings.

Grant, D.N. Blandon, C.A. and Priestley, M.J.N. (2004). Modelling Inelastic Response in Direct Displacement-Based Design, IUSS Press Pavia, Italy.

Nelder, J.A. and Mead, R. (1965). Downhill simplex method on multi-dimensional minimization, *Computer Journal*, **7**, 308

Paulay, T. and Priestley, M.J.N. (1992). Seismic Design of Reinforced Concrete and Masonry Buildings, John Wiley and Sons, Inc.

Paulay, T. (2002). A Displacement-Focused Seismic Design of Mixed Building Systems, *Earthquake Spectra*, **18:4**, 689-718.

Paulay, T. (2003). Seismic Displacement Capacity Of Ductile Reinforced Concrete Building Systems, *Bullettin of the New Zealand society for Earthquake Engineering*, **36:1**.

Priestley, M.J.N. (2003). Myths and Fallacies in Earthquake Engineering, Revisited, The Ninth Mallet Milne Lecture, IUSS Press, Pavia, Italy.

Priestley, M.J.N. and Grant, D.N. (2005). Viscous Damping, in Seismic Design and Analysis, *Journal of Earthquake Engineering*, **9:Special Issue 2**, 229-255.

Priestley, M.J.N. Calvi, G.M. and Kowalsky, M.J. (2007). Displacement-Based Seismic Design of Structures, IUSS Press, Pavia, Italy.

Sullivan, T.J. Priestley, M.J.N. and Calvi, G.M. (2005). Development of an Innovative Seismic Design Procedure for Frame-Wall Structures, Journal of Earthquake Engineering, **9:Special Issue 2**, 279-307.